ISSN 1063-7834, Physics of the Solid State, 2020, Vol. 62, No. 1, pp. 153–159. © Pleiades Publishing, Ltd., 2020.
Russian Text © The Author(s), 2020, published in Fizika Tverdogo Tela, 2020, Vol. 62, No. 1, pp. 110–116.

MAGNETISM

Ferromagnetic and Spin-Wave Resonance in the $[CoFe/Cu]_N$ Superlattice Thin (30-nm) Film

I. G. Vazhenina[a, *], R. S. Iskhakov[a], M. V. Rautskii[a], M. A. Milyaev[b], and L. I. Naumova[b]

[a] *Kirensky Institute of Physics, Krasnoyarsk Scientific Center, Siberian Branch, Russian Academy of Sciences, Krasnoyarsk, 660036 Russia*

[b] *Mikheev Institute of Metal Physics, Ural Branch, Russian Academy of Sciences, Yekaterinburg, 620108 Russia*

**e-mail: irina-vazhenina@mail.ru*

Received July 8, 2019; revised July 8, 2019; accepted July 16, 2019

Abstract—Angular dependences of the microwave absorption spectra of a $(CoFe/Cu)_N$ multilayer film have been studied by the ferromagnetic and spin-wave resonance techniques. The critical angle θ_c indicating the ranges of excitation of uniform and nonuniform spin modes, type of the boundary conditions, and surface anisotropy and exchange coupling constants have been established. It is shown that the accuracy of identification of individual modes in the spectra plays a key role in the analysis of the detected curves.

Keywords: ferromagnetic and spin-wave resonance, surface anisotropy constant, exchange coupling constant, superlattice

DOI: 10.1134/S1063783420010357

1. INTRODUCTION

The ferromagnetic resonance (FMR) and spin-wave (SWR) resonance techniques are well known to be reliable tools for determining the fundamental parameters of magnetic materials, including effective magnetization M_{eff}, exchange coupling constant A in the wave vector range of $k = (1–20) \times 10^5$ cm^{-1}, spin-wave stiffness η, and surface anisotropy constant K_S. The objects of study can be materials of different classes, e.g., thin ferromagnetic films [1–5], powder systems [6, 7], diluted magnetic semiconductors [8, 9], ferromagnetic metal–dielectric nanocomposites [10–12], and biological and chemical ferrihydride nanoparticles [13, 14]. Angular dependences of the resonance fields at both the perpendicular and parallel orientation of dc magnetic field H relative to the thin film plane provide information on the presence and value of the contributions of different anisotropies (magnetocrystalline, magnetoelastic, and surface) [8, 15–17].

The accuracy of determination of the above-mentioned magnetic parameters depends, to a great extent, on the accuracy of determination of the FMR field and correctness of identification of modes detected in the nonuniform FMR. In particular, the analysis of microwave absorption spectra of thin films must take into account a number of parameters, including the boundary conditions [18–21] and ferromagnetic film thickness [22], which affects the ratio between the intensities of the surface and standing spin wave modes, and, in the case of multilayer films, their composition [23–26], which determines the distribution of a magnetic parameter over the film thickness, and structural parameters (thickness and number of layers) [3, 27]. The rules of numbering the standing spin modes detected in the SWR spectrum were described in detail in [3, 22, 28–31].

Taking into account the above-mentioned factors in the analysis of the detected microwave absorption spectra, we established the main magnetic characteristics of the $[CoFe/Cu]_N$ superlattice in the form of a thin (~30 nm) film using the FMR and SWR techniques.

2. EXPERIMENTAL

A multilayer film in the form of a $[(Co_{0.88}Fe_{0.12})/Cu]_N$ superlattice containing a nonmagnetic spacer with a thickness of $t_s = 2.05$ nm was synthesized by magnetron sputtering on an MPS-4000-C6 facility and represented a planar nanostructure with the composition shown in Fig. 1a. The substrate used was Corning glass and the nonmagnetic Cu layer thickness was chosen to implement the second antiferromagnetic maximum of the exchange coupling of the CoFe layers through the Cu layer in the film system.

The structural measurements performed on a DRON-3M diffractometer in CoK_α radiation showed that the superlattice has a perfect layer structure with an fcc lattice and the ⟨111⟩ axial texture with the axis along the layer plane normal.

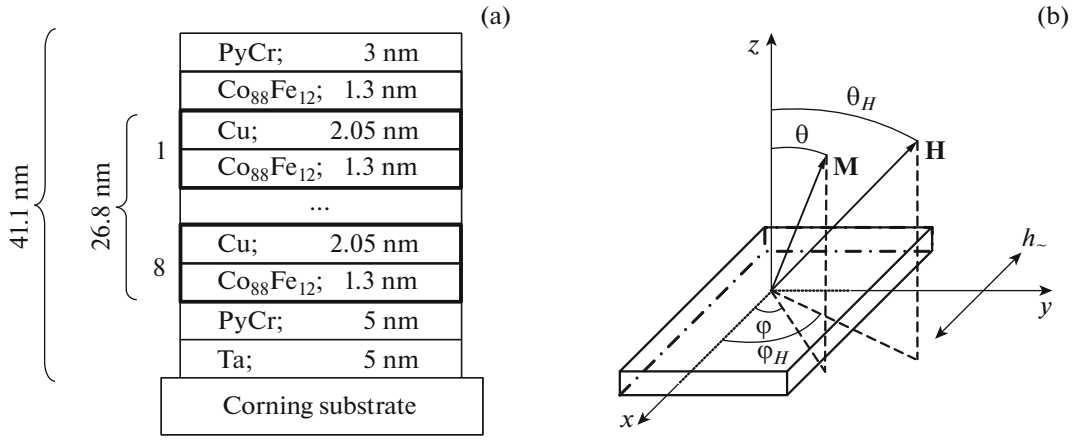

Fig. 1. (a) Composite structure of the sample and (b) experimental geometry.

The microwave spectra of the films were obtained on a Bruker ELEXSYS E580 spectrometer (Germany) at the Center for Collective Use of the Krasnoyarsk Scientific Center, Siberian Branch, Russian Academy of Sciences. The microwave spectra were measured at room temperature in the X range at a resonator pump frequency of $f = 9.2$ GHz; the sample was placed in the antinode of ac magnetic field $h_{\sim}$ of the cavity. The measurements were performed in the dc magnetic field $\bar{H}$ directed in the film plane (angle φ_n) and in the plane parallel to the film normal (angle θ_n) (Fig. 1b).

3. EXCITATION OF THE EXCHANGE SPIN WAVES IN THIN FERROMAGNETIC FILMS

The spin (magnetization) waves can have, depending on the boundary conditions, two types of distribution over the thin ferromagnetic film thickness. The first type is the uniform precession of the magnetization vector observed experimentally at the FMR and the second type is the standing exchange spin waves detected by the SWR technique.

The general expression for the FMR frequency ω_0 in the spherical coordinate system [16, 17, 32] in terms of the total energy E of a magnetic system can be presented, according to the Landau–Lifshitz equation for the motion of magnetization M specified by the polar (θ) and azimuthal (φ) angles, in the form

$$\omega_0 = \frac{\gamma}{M\sin\theta}\left[\frac{\partial^2 E}{\partial\theta^2}\frac{\partial^2 E}{\partial\varphi^2} - \left(\frac{\partial^2 E}{\partial\theta\partial\varphi}\right)^2\right]^{1/2}, \qquad (1)$$

where $\gamma = 1.758 \times 10^7$ Hz/Oe is the gyromagnetic ratio.

In this case, the equilibrium position of the magnetization vector is determined by the relation

$$\frac{\partial E}{\partial\varphi} = \frac{\partial E}{\partial\theta} = 0 \qquad (2)$$

and the free energy density is

$$\begin{aligned} E = &-MH[\sin(\theta)\sin(\theta_H)\cos(\varphi-\varphi_H) \\ &+ \cos(\theta)\cos(\theta_H)] \\ &+ \frac{K_1}{4}[\sin^4(\theta)\sin^2(2\varphi) + \sin^4(2\theta)] \\ &+ \frac{K_2}{16}\sin^2(2\theta)\sin^2(\theta)\sin^2(2\varphi) \\ &+ [2\pi M^2 + K_n]\cos^2(\theta) + K_u\sin^2(\theta)\sin^2(\varphi-\varphi_0), \end{aligned} \qquad (3)$$

where θ_H and φ_H are the polar and azimuth angles of the external dc magnetic bias H, K_1 and K_2 are the first and second cubic anisotropy constants, K_n is the perpendicular uniaxial anisotropy constant, and K_u is the constant of the in-plane uniaxial anisotropy acting at angle φ_0.

Solving numerically the system of equations (1), (2), and (3), we can find the resonance field H_0 of the uniform mode for an arbitrary external magnetic field direction. The limiting cases for a magnetically isotropic sample in the form of an infinitely thin disk obtained by Kittel in [33] are

$$\begin{aligned} &\frac{\omega_0}{\gamma} = (H_0 - 4\pi M_{\text{eff}}) \quad (\text{at} \quad \theta = \theta_H = 0^\circ), \\ &\left(\frac{\omega_0}{\gamma}\right)^2 = H_0(H_0 + 4\pi M_{\text{eff}}) \quad (\text{at} \quad \theta = \theta_H = 90^\circ), \end{aligned} \qquad (4)$$

where M_{eff} is the effective magnetization.

The angular dependence of the nonuniform self-oscillations of the magnetization (standing exchange spin waves) excited by uniform ac magnetic field h ($\mathbf{h} \perp \mathbf{H}$) with frequency ω is expressed as [34]

$$\left(\frac{\omega_0}{\gamma}\right)^2 = \left(H\sin\theta_H + 4\pi M\sin\theta + \frac{2Ak^2}{M}\sin\theta\right)$$

$$\times\left(H\sin\theta_H+\frac{2Ak^2}{M}\sin\theta\right) \quad (5)$$

$$+\left(H\cos\theta_H-4\pi M\cos\theta+\frac{2Ak^2}{M}\cos\theta\right)^2,$$

where A is the exchange coupling constant and k is the wave vector parallel to the film normal, which is determined by the exchange boundary conditions on the film surfaces.

The action of a dc magnetic field in the plane coinciding with the film surface normal ($\theta = \theta_H = 0°$) reduces Eq. (5) to the dependence of the resonance field positions on the wave vector described by Kittel [18]:

$$H_n=\frac{\omega}{\gamma}+4\pi M_{\text{eff}}-\frac{2A}{M_S}k^2. \quad (6)$$

A decisive factor in the excitation of standing spin waves is the boundary conditions. Assuming that the surface spins are generally pinned differently on different film surfaces, we can present the exchange boundary conditions as [22, 28, 29]

$$\left(\frac{\partial\mathbf{m}}{\partial z}+\beta_1^S\mathbf{m}\right)_{z=L/2}=0,\quad \left(\frac{\partial\mathbf{m}}{\partial z}-\beta_2^S\mathbf{m}\right)_{z=-L/2}=0, \quad (7)$$

where m is the complex amplitude of the variable magnetization; β_1^S and β_2^S are the parameters of surface spin pinning on different film surfaces, which are related to the surface anisotropy constant as $\beta^S=\frac{K_S}{A}$; and L is the film thickness.

The surface spin pinning parameter β^S and, consequently, the surface anisotropy constant K_S can take both positive and negative values. At $K_S > 0$ (the easy axis of the surface anisotropy is normal to the film surface), only the harmonic SWR modes with real values of the wave vector k are excited. At $K_S < 0$ (the hard axis of the surface anisotropy is normal to the film surface), along with the harmonic oscillations, a hyperbolic nonpropagating exchange spin wave (surface mode) with an imaginary wave vector is detected in the SWR spectrum. At $K_S = 0$, a uniform ac magnetic field $h_\sim(\mathbf{k}\perp\mathbf{H})$ only excites the uniform magnetization oscillation $\mathbf{m}_0\perp\mathbf{M}$ (FMR), since all the other possible $m(z)$ oscillations have a zero dipole moment.

According to [18], at the symmetric boundary conditions with $K_S=\infty$, the allowed values are $k=\frac{\pi n}{L}$, where n is the number of a trigonometric mode, which takes values of 1, 3, 5, 7, ... The form of the SWR spectrum at the antisymmetric boundary conditions, when the easy-axis pinning type is implemented on one surface and the hard-axis type, on the other surface, is determined by the ratio of $K_{S1} + K_{S2}$. The first possible variant is $|K_{S1}| = |K_{S2}|$, when the detected spectrum includes one surface mode in fields stronger than the field of the main trigonometric maximum and no even modes [35]. In the second variant, the $|K_{S1}|$ and $|K_{S2}|$ values are essentially different [36]. In the third variant, the sum $K_{S1} + K_{S2}$ [37] is slightly different from zero, which leads to the absence of an even mode with $n = 2$ in the spectrum. In addition, two surface modes can be detected in the SWR spectrum, which corresponds to the conditions $K_{S1} < 0$ and $K_{S2} < 0$. This pinning type is determined by the average magnetic moment on the surface and magnetization distribution over the film thickness [38].

4. RESULTS AND DISCUSSION

The form of the experimental microwave absorption spectra at angles from 20° to 90° is shown in Fig. 2 and, at angles from 0 to 10°, in Figs. 3 and 4.

Each resonance curve in the angular range from 20° to 90° is identified by us as a result of the excitation of a uniform mode ($k = 0$). The experimental resonance fields obtained in this range of angles θ_H coincide with a fairly high accuracy with the theoretical curve calculated by solving system of equations (1)–(3) (Fig. 5). At $\theta = \theta_H = 90°$, Eq. (4) yields a value of $M_{\text{eff}} \approx 1000$ G.

The complex microwave absorption curves in the angular range from 0 to 10° (Figs. 3 and 4) were decomposed into components using the differentiated Lorentz function, which was chosen with regard to the zero electric component contribution caused by the resonator design and sample size. An example of the decomposition is presented in Fig. 4b.

The modes observed in the microwave spectrum in the angle range of $15° < \theta_H < -15°$ are identified by us as two surface (the easy plane boundary conditions at $-K_{S1} \neq -K_{S2}$) and a standing exchange spin wave ($n = 1$). The dependence of the mode type (uniform or nonuniform) on the angle θ_H was observed as early as in the first decade after the discovery of the SWR phenomenon [34]. Wigen et al. [34] not only determined the angular dependence of the resonance fields on the angle θ_H (Eq. (5)), but also established the conditions under which the critical angle $\theta_{H\text{critic}}$ of the transition from the nonuniform to uniform mode can be found. Using Eq. (5), a value of $M_{\text{eff}} \approx 1000$ G, and the conditions described in [34], we calculated the $\theta_{H\text{critic}}$ value, which was found to be $15° \pm 2°$ in the range of the field magnetization angle θ from 0° to 25°. The angle at which the experimental curve of the microwave spectrum becomes composite coincides with $\theta_{H\text{critic}}$ (Fig. 5).

A factor important for the interpretation of the spectra was the intensity of selected modes. The intensity of the nonuniform spin modes depends on the sample thickness and the value and sign of the surface anisotropy constant [21]. The behavior of the angular dependence is determined by the deviation of the uni-

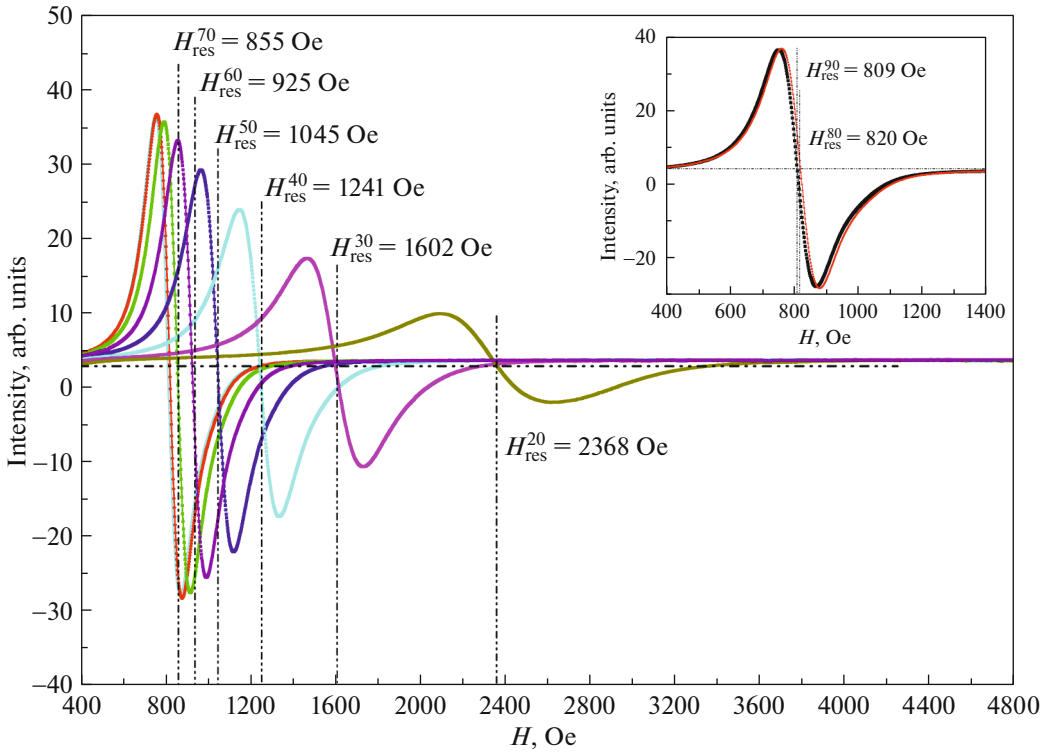

Fig. 2. Experimental spectra in the range from 20° to 90° (the resonance field superscript marks the value of angle θ_H).

axial anisotropy field from the film normal [39, 40]. The study of the dependence between the intensity I_1 of the first bulk mode and the intensity I_S of the surface mode on the film thickness [22] showed that, in films with a thickness of smaller than 100 nm, we have $I_S > I_1$ and the dominance of I_S over I_1 starts manifesting especially strong when the dc magnetic field deviates from the film normal. The significance of the contribution of the film thickness to the mode intensity distribution in the SWR spectrum can be demonstrated by the example of study [41], the authors of which indicated the highest intensity peak in the SWR spectrum of an ultrathin (50-nm) FePt film as a uniform resonance mode and the lower-intensity peak, as the first bulk standing mode. Based on the identification, they determined the spin-wave stiffness η, which appeared to be overestimated. The estimated K_S at the identification of the spectrum as the excitation of the surface and first bulk modes agrees well with the results of [42], where the authors determined the K_S value using the Néel model.

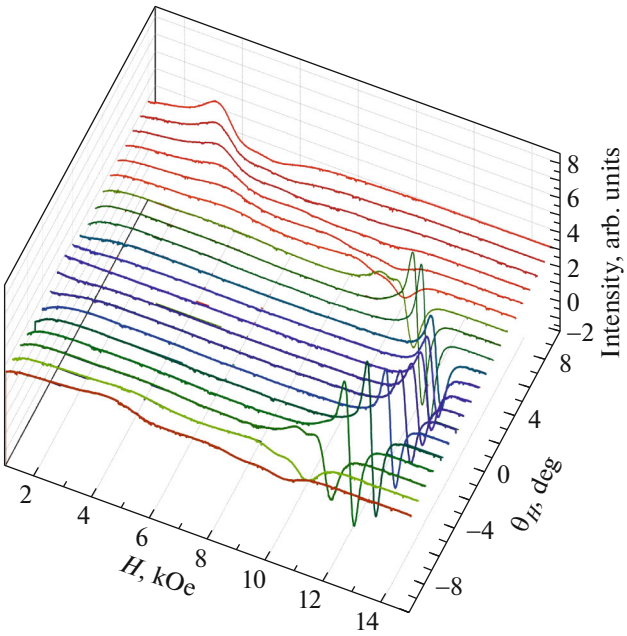

Fig. 3. Field distribution of the experimental spectra in the angular range from 10° to −10°.

The film under study has a total magnetic layer thickness of ~30 nm; therefore, the inequality $I_S > I_1$ should be valid, which was taken into account when identifying the processed spectra. The decomposition of the experimental spectra into constituent modes allowed us to obtain the dependence of the mode intensities on the angle θ_H (Fig. 6).

As was mentioned above, the form of the angular dependence of the intensity, as was theoretically established in [39] and experimentally confirmed in [40], is

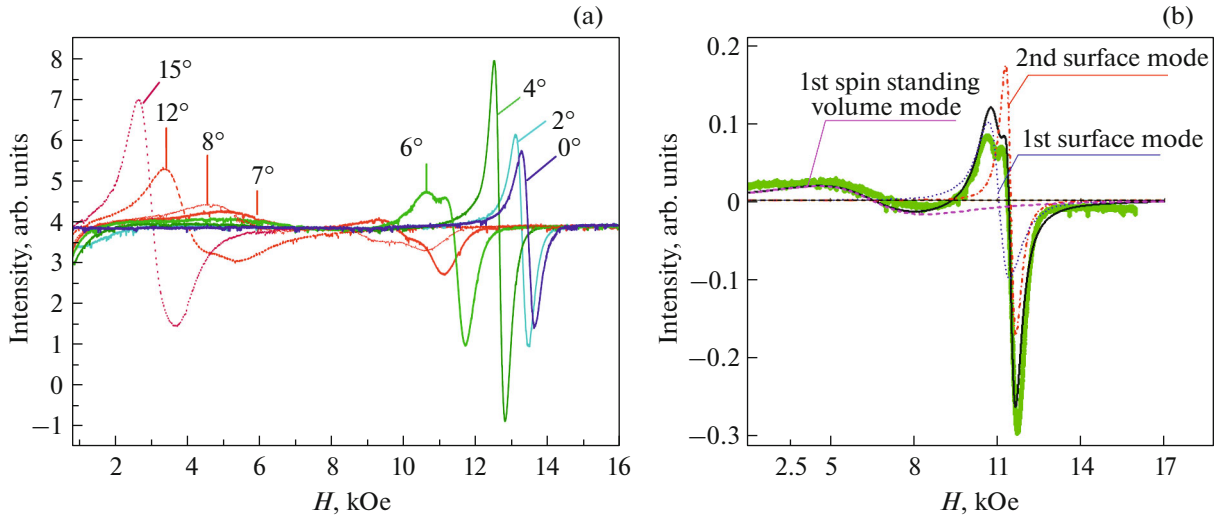

Fig. 4. (a) Separate experimental spectra in the range from 15° to 0°. (b) Example of decomposition of the experimental spectrum into Lorentzians at $\theta_H = 6°$.

determined by the angle of deviation of the anisotropy field from the film normal.

The maximum intensity of the surface modes (Fig. 6) corresponds to 4° and 6°; therefore, there is the deviation of the normal anisotropy field from the normal by an angle of ~5°. The assumption about the deviation of the surface anisotropy axis is grounded on several facts. First, this is the absence of uniaxial anisotropy in the film plane, which is confirmed by the dependences of the resonance fields on the angle φ_H at $\theta_H = 90°$. Second, this is the form of the angular dependence of the intensity I_0 of the uniform mode, which gradually increases upon variation in the angle θ_H from 20° to 90°. A similar change in the $I_0(\theta_H)$ occurs when the angle of the uniaxial perpendicular anisotropy coincides with the film normal and the angle of deviation of the surface anisotropy field from $\theta_H = 0°$ is small. A possible reason for the deviation of the surface anisotropy field axis may be the formed ⟨111⟩ axial texture.

The presence of surface modes in the spectrum makes it possible to determine the surface anisotropy constant, which, at $K_S < 0$, is calculated using the formula

$$|K_S| = \left[\frac{M_{\text{eff}}A}{2}\left[(H_S - H_1) - \frac{2A}{M_{\text{eff}}}\left(\frac{\pi}{L}\right)^2\right]\right]^{1/2} \quad (8)$$

and, at the symmetric boundary conditions K_S, can be estimated as [43]

$$K_S = \frac{n^2\pi}{2}\frac{A}{2}\frac{\Delta H_n}{\Delta H_S}\sqrt{\frac{I_n}{I_S}}, \quad (9)$$

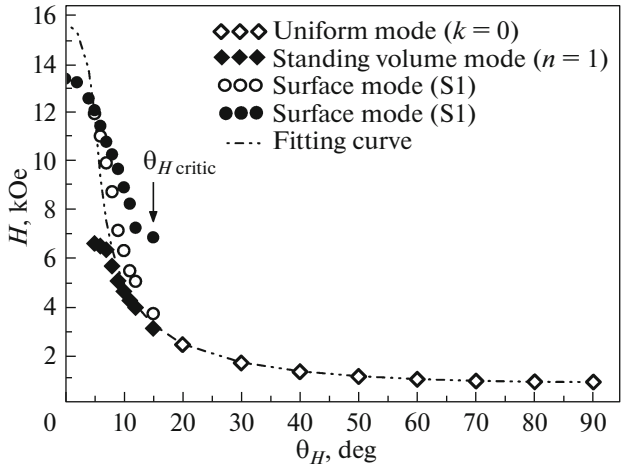

Fig. 5. Angular dependence of the resonance field positions.

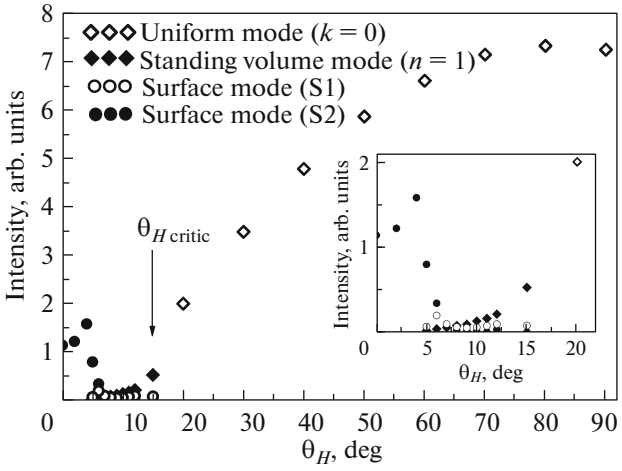

Fig. 6. Angular dependence of the intensities of individual modes.

where ΔH_n is the linewidth of the nth bulk standing spin mode and ΔH_S is the surface mode linewidth.

The joint solution of Eqs. (8) and (9) allows us to estimate the quantities A, $|K_{S1}|$, and $|K_{S2}|$, where $S1$ and $S2$ are the first and second surface modes, as ~0.2 × 10^{-6} erg/cm, ~0.24 erg/cm^2, and ~0.54 erg/cm^2, respectively. The numerical value of the exchange coupling constant is consistent with the data from [44], where the authors established the effect of the ratio between the thicknesses of the magnetic and nonmagnetic layers on the A value.

5. CONCLUSIONS

The investigations of the dynamic characteristics of the $[CoFe/Cu]_N$ multilayer film showed the possibility of using the FMR and SWR techniques for determining the fundamental magnetic parameters and identifying the structural features. The detected microwave absorption spectra and their angular dependences made it possible to establish the type of boundary conditions (the easy plane on both surfaces of the standing spin wave pinning) and estimate the surface anisotropy field constants as $K_{S1} = -0.24$ erg/cm^2 and $K_{S2} = -0.54$ erg/cm^2, the presence of a deviation of the surface anisotropy field from the film normal, and the angle of this deviation (~5°).

The implementation of the nonuniform spin waves at the perpendicular orientation of the film in a dc magnetic field allowed us to determine the exchange coupling constant to be ~0.2 × 10^{-6} erg/cm. The ranges of the angle θ_H corresponding to the excitation of the uniform and nonuniform modes of spin waves were established.

FUNDING

This study was supported by the Russian Foundation for Basic Research, Government of the Krasnoyarsk Krai, and Krasnoyarsk Territorial Foundation for Support of Scientific and R&D Activities, project no. 18-42-243005 "Synthesis and Study of the Magnetic Properties of Gradient Materials with Different Types of a Specified Magnetic Parameter" and project "Spin" no. AAAA-A18-118020290104-2.

CONFLICT OF INTEREST

The authors declare that they have no conflicts of interest.

REFERENCES

1. V. V. Kruglyak, C. S. Davies, V. S. Tkachenko, O. Yu. Gorobets, Yu. I. Gorobets, and A. N. Kuchko, J. Phys. D **50**, 094003 (2017).
2. A. I. Stognij, L. V. Lutsev, V. E. Bursian, and N. N. Novitskii, J. Appl. Phys. **118**, 023905 (2015).
3. R. S. Iskhakov, S. V. Stolyar, M. V. Chizhik, and L. A. Chekanova, JETP Lett. **94**, 301 (2011).
4. D. M. Jacobi, E. Sallica Leva, N. Álvarez, M. Vásquez-Mansilla, J. Gómez, and A. Butera, J. Appl. Phys. **111**, 033911 (2012).
5. I. G. Vazhenina, R. S. Iskhakov, and L. A. Chekanova, Phys. Solid State **60**, 292 (2018).
6. G. Thirupathi and R. Singh, AIP Conf. Proc. **1665**, 050133 (2015).
7. L. A. Kuzovnikova, E. A. Denisova, S. V. Komogortsev, I. V. Nemtsev, R. S. Iskhakov, L. A. Chekanova, and V. K. Mal'tsev, Bull. Russ. Acad. Sci.: Phys. **81**, 295 (2017).
8. L. Dreher, C. Bihler, E. Peiner, A. Waag, W. Schoch, W. Limmer, S. T. B. Goennenwein, and M. S. Brandt, Phys. Rev. B **87**, 224422 (2013).
9. A. I. Dmitriev, R. B. Morgunov, O. L. Kazakova, and J. Tanimoto, J. Exp. Theor. Phys. **108**, 985 (2009).
10. A. Butera, J. N. Zhou, and J. A. Barnard, Phys. Rev. B **60**, 12270 (1999).
11. E. A. Denisova, S. V. Komogortsev, R. S. Iskhakov, L. A. Chekanova, A. D. Balaev, Yu. E. Kalinin, and A. V. Sitnikov, J. Magn. Magn. Mater **440**, 221 (2017).
12. X. Liu and J. K. Furdyna, J. Phys.: Condens. Matter **18**, R245 (2006).
13. D. A. Balaev, A. A. Krasikov, A. A. Dubrovskiy, S. I. Popkov, S. V. Stolyar, O. A. Bayukov, R. S. Iskhakov, V. P. Ladygina, and R. N. Yaroslavtsev, J. Magn. Magn. Mater **410**, 171 (2016).
14. S. V. Stolyar, R. N. Yaroslavtsev, R. S. Iskhakov, O. A. Bayukov, D. A. Balaev, A. A. Dubrovskii, A. A. Krasikov, V. P. Ladygina, A. M. Vorotynov, and M. N. Volochaev, Phys. Solid State **59**, 555 (2017).
15. A. Layadi, Phys. Rev. B **66**, 184423 (2002).
16. J. Smit and H. G. Beljers, Philips Res. Rep. **10**, 113 (1955).
17. J. O. Artman, Phys. Rev. **105**, 74 (1957).
18. C. Kittel, Phys. Rev. **110**, 1295 (1958).
19. W. S. Ament and G. T. Rado, Phys. Rev. **97**, 1558 (1955).
20. H. Puszkarski, Prog. Surf. Sci. **9**, 191 (1979).
21. H. Puszkarski and P. Tomczak, Surf. Sci. Rep. **72**, 351 (2017).
22. Yu. A. Korchagin, R. G. Khlebopros, and N. S. Chistyakov, Fiz. Met. Metalloved. **34**, 1303 (1972).
23. A. M. Portis, Appl. Phys. Lett. **2** (4), 69 (1963).
24. E. Schlömann, J. Appl. Phys. **36**, 1193 (1965).
25. R. S. Iskhakov, L. A. Chekanova, and I. G. Vazhenina, Bull. Russ. Acad. Sci.: Phys. **77**, 1265 (2013).
26. V. A. Ignatchenko and D. S. Tsikalov, in *Proceedings of the 6th Euro-Asion Symposium on Trends in MAGnetism* (Kirensky Inst. Phys., Krasnoyarsk, 2016), p. 264.
27. R. S. Iskhakov, S. V. Stolyar, L. A. Chekanova, and M. V. Chizhik, Phys. Solid State **54**, 748 (2012).
28. Yu. A. Korchagin, R. G. Khlebopros, and N. S. Chistyakov, Sov. Phys. Solid State **14**, 1826 (1972).
29. N. M. Salanskii and M. Sh. Erukhimov, *Physical Properties and Application of Magnetic Films* (Nauka, Novosibirsk, 1975) [in Russian].

30. A. G. Gurevich, *Magnetic Resonance in Ferrites and Antiferromagnets* (Nauka, Moscow, 1973) [in Russian].
31. V. M. Sokolov and B. A. Tavger, Sov. Phys. Solid State **10**, 1412 (1968).
32. H. Suhl, Phys. Rev. **97**, 555 (1955).
33. C. Kittel, Phys. Rev. **73**, 155 (1948).
34. P. E. Wigen, C. F. Kooi, M. R. Shanabarger, U. K. Cummings, and M. E. Baldwin, J. Appl. Phys. **34**, 1137 (1963).
35. R. S. Iskhakov, M. M. Brushtunov, and L. A. Chekanova, Sov. Phys. Solid State **29**, 1553 (1987).
36. R. S. Iskhakov, M. M. Brushtunov, A. G. Narmonev, I. A. Turpanov, and L. A. Chekanova, Fiz. Met. Metalloved. **79**, 122 (1995).
37. V. A. Ignatchenko, R. S. Iskhakov, L. A. Chekanova, and N. S. Chistyakov, Sov. Phys. JETP **48**, 328 (1978).
38. J. T. Yu, R. A. Turk, and P. E. Wigen, Phys. Rev. B **11**, 420 (1975).
39. A. Layadi, Phys. Rev. B **63**, 174410 (2001).
40. J. A. Hagmann, K. Traudt, Y. Y. Zhou, X. Liu, M. Dobrowolska, and J. K. Furdyna, J. Magn. Magn. Mater **360**, 137 (2014).
41. C. Antoniak, J. Lindner, K. Fauth, J.-U. Thiele, J. Minár, S. Mankovsky, H. Ebert, H. Wende, and M. Farle, Phys. Rev. B **82**, 064403 (2010).
42. E. Burgos, E. Sallica Leva, J. Gómez, F. Martínez Tabares, M. Vásquez Mansilla, and A. Butera, Phys. Rev. B **83**, 174417 (2011).
43. A. Stankov, in *Physics of Magnetic Films, Collection of Articles*, Ed. by. M. G. Rubashevskaya (Vost.-Sib. Pravda, Irkutsk, 1968), p. 422 [in Russian].
44. R. S. Iskhakov, N. A. Shepeta, S. V. Stolyar, L. A. Chekanova, and V. Yu. Yakovchuk, JETP Lett. **83**, 28 (2006).

Translated by E. Bondareva